American Journal of Environment and Climate (AJEC)

ISSN: 2832-403X (ONLINE)

VOLUME 4 ISSUE 2 (2025)

PUBLISHED BY
E-PALLI PUBLISHERS, DELAWARE, USA

American Journal of Environment and Climate (AJEC)

Volume 4 Issue 2, Year 2025
ISSN: 2832-403X (Online)
DOI: https://doi.org/10.54536/ajec.v4i2.4518
https://journals.e-palli.com/home/index.php/ajec

Quantifying Extreme Rainfall Events and Hydrologic Modeling for Flood-Resilient Bridge Design in Kano, Nigeria

Oluwatobi Oluwaseun Aiyelokun[1*], Adewoye Alade Olanipekun[2], Oluwole Akinyele Agbede[1], Quadri Opeyemi Saka[3], Damilare Akintunde Ojewole[3]

Article Information

Received: February 15, 2025
Accepted: March 17, 2025
Published: June 25, 2025

Keywords

Bridge Design, Climate Change, Hydrologic Modeling, Rainfall

ABSTRACT

Climate change and some of its impacts (irregular rainfall and flooding) negatively affect hydraulic structures, especially in regions at risk of extreme weather conditions. Thus, it is critical to incorporate robust weather data in the design of hydraulic structures such as bridges. Therefore, this study evaluated extreme rainfall events and their implications for hydrologic and hydraulic modeling at a proposed bridge site in Kano, Nigeria. Analysis of 2001–2019 rainfall data revealed annual maximum rainfall ranging from 44.43 mm to 114.89 mm, with a mean of 82.67 mm and a standard deviation of 19.22 mm, exhibiting a positively skewed distribution. Frequency analysis using Hazen plotting positions estimated the largest observed storm (114.90 mm) to have a 19-year return period, with projected rainfall intensities reaching 135.45 mm, 174.83 mm and 212.67 mm for 50, 100 and 500-year return periods, respectively. Goodness-of-fit (GOF) tests identified the log-normal distribution as the best fit for estimating design storms. Intensity-Duration-Frequency (IDF) analysis disaggregated 24-hour rainfall into durations as short as 10 minutes, yielding peak intensities of 67.89 mm/hr for 2-year events and 221.34 mm/hr for 1000-year events. Hydrologic modeling incorporating catchment characteristics such as curve numbers, slopes, and basin areas simulated peak discharges of 78.34 m^3/s, 142.67 m^3/s and 186.45 m^3/s for 2-year, 50-year and 100-year events, respectively at the proposed bridge location. The findings underscore the importance of robust rainfall modeling and hydrologic analysis in designing flood-resilient infrastructure, especially in regions susceptible to extreme weather events.

INTRODUCTION

The scientific study of the ongoing movement, control, and distribution of water on Earth is known as engineering hydrology. The design, building, and upkeep of engineering structures (open or closed channels) necessary for properly distributing treating, retaining and transporting water or other fluids is known as hydraulics engineering (Nwaogozie & Ekwueme, 2017). When it rains, the nearby trees' stems and leaves typically catch the first drops of water that fall. This phenomenon is frequently referred to as interception storage. But as the downpour persists, the water that reaches the land starts to seep into the soil, until the rainfall volume surpasses the soil's ability to absorb it (Akpan & Okoro, 2013). As a result, ditches, surface puddles, and other existing surface depressions are filled (depression storage), eventually resulting in surface runoff (Oladejo, 2014).

Sule & Ige (2016) claimed that the structure and the soil moisture content (dependent on the previous dry or rainfall season) greatly determine the infiltration capacity of the soil. Moreover, a dry soil has a large initial infiltration capacity, but as the rainfall keeps on, the capacity reduces continuously until it achieves the final infiltration rate. Therefore, surface runoff generation will keep on if the rainfall intensity surpasses the soil's infiltration capacity and will similarly end right away the rainfall intensity falls below the infiltration rate. Studies have verified that surface runoff generation could become a major environmental issue particularly in communities where drainages, culverts, bridges and other water holding structures which should channel the runoff generated into surface water bodies have not been sufficiently provided (Obot *et al.*, 2010; Antigha & Ogarekpe, 2013).

According to Oladejo & Olanipekun (2018) asserted that the pools of water created become breeding grounds for disease vectors when ditches and surface puddles are filled up following rainfall without a sufficient channel through which the water will be transported, so putting the residents of such communities effectively at risk of waterborne diseases. Furthermore, such pools of water begin to create bad odour as a result of facultative bacteria feeding on the water's limited dissolved oxygen, thereby decreasing the community's standard of life (Olanipekun & Idusuyi, 2023). Studies have revealed that these conditions are the result of inadequate environmental and settlement planning, which is widespread impoverished and developing countries such as Nigeria. Residents of such communities endure multiple cases of waterborne infections each year, compared with developed countries with superior environmental planning practices norms (Fadipe *et al.*, 2020; World Health Organization, 2022).

Thus third-world countries must address this environmental anomaly by investing enough resources in the design, construction, and maintenance of hydrological and hydraulic structures for water channelization.

[1] Department of Civil Engineering, University of Ibadan, Nigeria
[2] Department of Civil and Environmental Engineering, Bells University of Technology, Ota, Nigeria
[3] Department of Mechanical Engineering, Bells University of Technology, Ota, Nigeria
[*] Corresponding author's e-mail: aiyelokuntobi@gmail.com

However, according to Ahmed *et al.* (2021), the design of hydraulic structures such as drainages, culverts, and bridges necessitates a complete study of available rainfall data using a valid statistical method, which highly trained technical professionals, carry out. This entails using appropriate stochastic methods to determine rainfall intensity (or depth), which is an important consideration when designing hydraulic structures. Hydrologic assessments give information on flood magnitudes and frequency, allowing for safe and cost-effective hydraulic structure design. An efficient and successful method for estimating design flood is flood frequency analysis (Rasel & Islam, 2015).

The method allows the user to estimate the probability that a certain hydrological event will occur by fitting a theoretical probability distribution to one that is empirically obtained from recorded data.

Furthermore, also mentioned by Adewale & Isaac (2017) are intensity-frequency (IDF) curves that define the relationship between rainfall intensity, duration, and return period or its inverse, likelihood of exceedance. Consequently, the design of hydrologic, hydraulic, and water resource systems makes regular use of IDF curves, often produced from frequency analysis of rainfall observations. Given this, this work calculated different design storm estimates and the associated discharges for five bridge crossings in Kano State of Nigeria. This was considered for varied durations and return periods using the best available probability distribution model and design flood estimation process.

The study developed IDF curves and design peak discharge at 100-year return periods to simplify the hydraulic analysis of the proposed bridge crossing. This was accomplished through the study's objectives, which included designating catchment regions for bridge crossings and outlets, developing the IDF core of the project area, and computing the 100-year design flood for the planned bridges in Kano State, Nigeria.

MATERIALS AND METHODS

Study Area and Hydrologic Modeling

This study was conducted in Kano, a city in Nigeria's northwest. According to Isah *et al.* (2020), the city resides in the latitude 12°00'00.00"N and longitude 8°51'40.00"E. It is also found between latitude 10°30'N and 13°N and longitude 7°40'E and 10°35'E. Kano is adjacent to the Sahara Desert, giving it dry and hot weather. However, the city sees both the dry and rainy seasons every year. The dry season lasts from October to April, while the rainy season lasts from May to September. Like other Northern cities, Kano has experienced severe flooding in the past, and it is considerably more vulnerable now due to climate change and the lack of flood-resistant construction in the majority of the city's hydraulic systems. The city contains scrub vegetation in the north and woodland savanna in the south. The Kano-Chalawa-Hadejia river system provides drainage for Kano. As a result, the following methods were used for hydrological and hydraulic simulation using design peak flood computation for bridge design in Kano State, Nigeria: extreme rainfall computation, probability distribution, goodness 25 of fit statistics and criteria, IDF curve generation, and hydrologic simulations. The hydrologic modeling and simulation of peak floods projected for the planned bridge crossings were also carried out using the United States Army Corps of Engineers, Hydrologic Engineering Centre - Hydrologic Modeling System (HEC-HMS) version 4.11.

Extreme Rainfall Computation

Using the Integrated Multi-Satellite Retrievals for GPM (IMERG), (https://gpm.nasa.gov/data/imerg), the World Weather for Water Data Service (W3S) produced 19 years of daily rainfall data from 2001 to 2019. The gathered data were used to create a set of one-day severe showers. Moreover, concise information about the produced series was given via statistical summaries comprising mean, standard deviation, skewness, and kurtosis. Hazen's plotting position computed the probability that the ranked maxima would be reached or exceeded for any return interval; the produced 1-day extremes were arranged in decreasing order of magnitude and shown in equation 1:

$$T_r=(m-0.5)/n \quad ....(1)$$

Where;

Tr is the return period, m is the order or rank and n is the number of years of study

Probability Distributions

Five probability distributions; Weibull, Gamma, Gumbel, Log-normal, and Normal—were chosen based on first analysis of the 1-day extreme rainfall data. The probability density functions (PDF) of Weibull, Gamma, Gumbel, Log-normal, and Normal distributions respectively are represented by equations 2, 3, 4, 5, and 6.

$$f(x;\alpha,\beta) = (\beta/\alpha)\,(\alpha/x)^{\beta+1}\, e^{-(\alpha/x)\beta}),\ -\infty < x < \infty,\ \alpha > 0 \quad ....(2)$$

$$f(x,\alpha,\beta) = (1/(\alpha^{\beta}\,\Gamma\beta))\, x^{\beta-1}\, e^{-(x/\alpha)}),\ x,\alpha,\beta > 0 \quad ....(3)$$

$$f(x;\alpha,\beta) = (e^{-(x-\beta)}/\alpha)\, e^{-e(-(x-\beta)/\alpha))}/\alpha,\ -\infty<x<\infty,\alpha>0 \quad ....(4)$$

$$f(x,\mu_y,\sigma_y) = \frac{1}{\sigma_y x\sqrt{2\pi}}\, e^{-\frac{1}{2}\left(\frac{\ln(x)-\mu_y}{\sigma_y}\right)^2},\quad x, y > 0 \quad ....(5)$$

$$f(x,\mu_x,\sigma_x) = \frac{1}{\sigma_x\sqrt{2\pi}}\, e^{-\frac{1}{2}\left(\frac{(x)-\mu_x}{\sigma_x}\right)^2},\quad x, y > 0 \quad ....(6)$$

Where;

the mean and standard deviation of the series of the annual extreme rainfall are represented by μy and σy, the scale and location parameters are shown by α and β respectively; the mean and standard deviation of the log-transformed series of annual extreme rainfall is shown by μy and σy. Furthermore, the distribution parameters were estimated in this work using the Maximum Likelihood Method (MOM). Hassan *et al.* (2019) provided a description of the equations and theoretical vocabulary for parameter estimate employing MOM of the selected distributions.

Goodness of Fit Statistics and Criteria

Along with GOF criteria, Akaike Information Criteria (AIC) and Bayesian Information Criteria (BIC), Kolmogorov-Smirnov (KS) test (Chowdhury *et al*., 1991), and Cramer-von Mises (CM) test (Arnold and Emerson, 2011) were used to evaluate the fit of the chosen probability distributions.

Anderson-Darling (Ad) Test

More often used for outlier detection, the AD test compares the cumulative distribution function of empirical and probability distributions. Equation 7 gives the AD test (A2);

$$A^2 = - N - (1/N)\sum^{N}_{i=1} (2i - 1)*(\ln F_e (Q_i) + (\ln(1-F_D (Q_i)) \quad ....(7)$$

Where;

The Anderson–Darling test statistic is A^2; Fe is the cumulative distribution function of the designated distribution; Qi is the ordered observed data.

Kolmogorov–Smirnov (Ks) Test

Equation 8 indicates the KS test, which is predicated on the highest vertical deviation between the cumulative distribution functions of the empirical and theoretical distributions.

$$KS = Max(F(Q_i) - ((i-1)/N), (i/N) F(Q_i)) \quad ....(8)$$

Where;

$F(Q_i)$ is the theoretical cumulative distribution of distribution being assessed.

Cramer-Von Mises (Cm) Test

Contrasting the first two GOF Statistics, the "CM test considers an observed hydrological time series in an increasing order" (Langat *et al*., 2019). This is represented in equation 9 accordingly;

$$W^2 = \sum^{N}_{i=1} (F(Q_i) - (i - 0.5)/N)^2 + 1/12N \quad ....(9)$$

Akaike Information Criterion

Regarding the established GOF criteria, the Akaike information criterion is extensively utilized for the selection of appropriate stochastic models, as delineated in equation 10;

$$AIC = n(\log\sigma^2 + 1) + 2p \quad ....(10)$$

Where;

σ^2 and p presents the variance and the parameter count of the subset stochastic model. AIC generally gives preference to models that minimize equation 10.

Bayesian Information Criterion (BIC)

BIC is intricately connected to AIC, as it is largely derived from the likelihood function and is expressed by equation 11 appropriately.

$$-2 \cdot \ln p(x \mid k) \approx BIC = -2 \cdot \ln L + k \ln(n) \quad ....(11)$$

Where;

L represents the maximum value of the likelihood function, p(x | k) denotes the probability or likelihood of parameters given the dataset, n signifies the sample size, k indicates the number of free parameters to be estimated, and x refers to the observed data.

The extremely efficient AD test was used for final selection when various goodness-of-fit statistics or criteria supporting multiple distributions were considered (Laio, 2004). The probability distribution with the lowest Anderson-Darling statistic and a cumulative distribution function closely resembling the actual distribution was selected. The adequacy of the distributions was additionally validated by a graphical or qualitative assessment method utilizing CDF plots.

Generation of IDF Curve

Rainfall intensity is the total amount of rainfall per time (rainfall depth). Usually, it is expressed in millimeters per hour, or inches per hour. Following the most suitable probability distribution for modelling the annual peak flood using the previous approaches, the disaggregated rainfall depth for lower rainfall durations longer than 24 hours was calculated using the empirical reduction formula supplied by the Indian Meteorological Department (IMD), as reported by Laboya & Nwachukwu (2022);

$$p_t = P_{24} (t/24)^{(1/3)} \quad ....(12)$$

Where;

P_{24} is the daily rainfall depth (mm); Pt is the required rainfall depth; t is the length of rainfall for which the rainfall depth is needed in (hr). Rainfall was calculated for eight periods: five minutes, fifteen minutes, thirty minutes, sixty minutes, one hundred and twenty minutes, one hundred and eighty minutes, three hundred and sixty minutes, seven hundred and twenty minutes, and one thousand four hundred and forty minutes. Subsequently, rainfall intensities were calculated for the calculated rainfall depths at specified periods using equation 13 as shown:

$$I = R/T \quad ....(13)$$

Where;

The rainfall intensity (mm/hr), R; is the total rainfall (mm); T; is the rainfall duration (hr).

Hydrologic Simulations

The procedures adopted for the hydrologic design calculations are presented accordingly;

Hydrologic design

The hydrological study aims to project the highest discharges that would pass across the bridge crossings. The study also took into account hydrology-related subjects including IDF development and other factors influencing the rainfall-runoff correlation.

Catchment basins delineation

The physiographical features of the upstream catchments were ascertained using the available satellite photos and elevation data in order to get all information concerning areas, elevations, slopes, and morphometric parameters, including information on main water course. Thereafter, it was clear where the catchment area of the watercourses boarding or crossing the proposed bridge locations rested. Moreover, the ArcMap GIS environment was used for the delineation of catchment areas; the five

catchments' boundaries were generated by using the HEC-geoHMS program feature of ArcMap GIS. Developing the catchment models started with defining the watershed limits and stream network of the area of interest. Usually referred to as terrain preprocessing, this method depends just on the input (Digital Elevation Model) DEM. Terrain preprocessing was done using a 12.5-metre pixel size developed by the Alaska Satellite Facility (ASF), a component of the University of Alaska Fairbanks (Alaska Satellite Facility, 2015), Advanced Land Observing Satellite/Phased Array type L-band Synthetic Aperture Radar (ALOS/PALSAR) DEM.

The following GRID files were derived from the DEM by following the step by step functionality of HEC-geoHMS.

• Fill Sinks GRID: Empty sinks Based on the input DEM, GRID generates a hydrologic-ally corrected DEM which are either depression-less or otherwise. The program also automatically raises any pit cell's elevation value to match the level of the surrounding terrain

• Flow Direction GRID: This GRID came from the Fill Sinks GRID. Every grid cell in the grid processing defines the direction of the sharpest fall to a neighboring cell

• Flow Accumulation GRID: Drawn from the flow direction GRID, this GRID specifies the number of upstream cells emptying into any specific grid cell

• Stream Definition GRID: This stage specified the stream network's constituent cells depending on a threshold count of cells that drain into a particular cell. The criteria for the definition of streams in this study was one percent of Ogun River Basin's overall area. The outcome was a GRID in which lines of connected grid cells all satisfy the threshold requirements, therefore representing the stream network

• Stream Segmentation GRID: Splitting the streams as stated in the stream definition GRID at any junction produces this GRID.

• Catchment Grid: Every stream segment identified by the stream segmentation GRID corresponds to a demarcated watershed kept in a GRID file

Three vector layers were produced depending on the results of these computational phases to finish the terrain preparation of the basin, comprising;

• Catchment Polygons: This utility defines the limits of every sub-basin using the catchment GRID as a vector layer.

• Drainage Line: This converts the defined stream segments based on the stream segmentation GRID into a vector stream layer.

• Adjoint Catchment: Here the upstream sub-basins are gathered at any stream confluence. Although it is not hydrologic-ally relevant, this stage improves the computational efficiency in the subsequent ones.

HEC-HMS methods and parameters

Using many computation methods, each with linked input parameters, the HEC-HMS model characterizes the hydrologic response process of a basin. Graphical representation of the HEC-HMS processes, methods, and associated parameters implemented for the research area are shown in Figure 1. This study however ignored base flow, canopy storage, surface depression storage and channel loss.

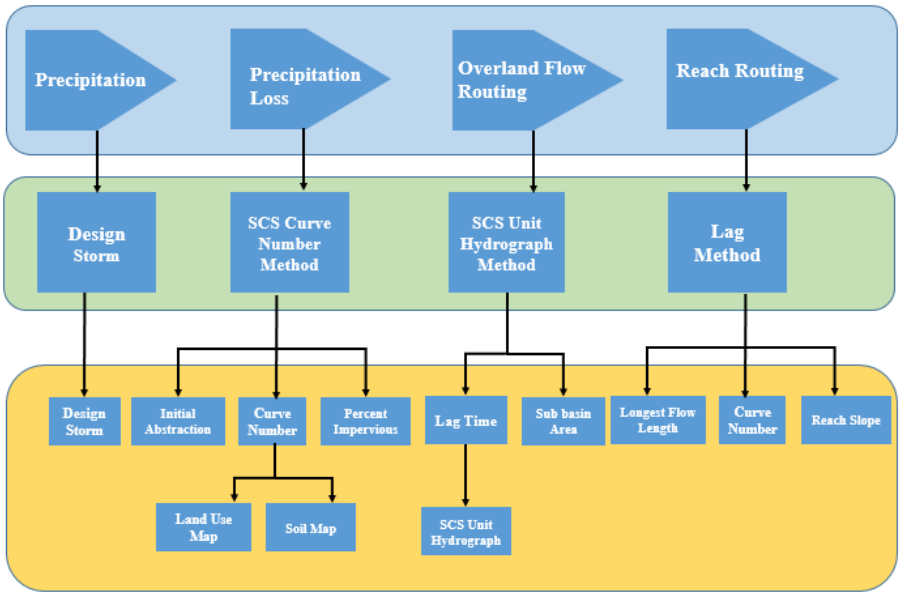

Figure 1: Summary of Processes, Methods, and Associated Data Requirements for HEC-HMS

Design storm

Conventional historical daily precipitation data for the project site was lacking, hence satellite-based data was chosen as described under extreme rainfall computation. Thus, the modeling of floods in HEC-HMS took advantage of the precipitation input in form of design storms produced from the created IDF curves. The frequency of a storm occurrence is the number of times

it passes during a given length of time. The frequency of storm events determines the probability of flooding and a low danger corresponds to a low frequency. Design frequency depends on the hydraulic system installation and the areas of catchment that need to be drained. Table 1 includes the recommended design storm frequency for the several hydraulic system components; since the hydrologic assessment was done for bridges, the study therefore used the design return period of one hundred years.

Table 1: Design Return Period

Type of System	Design Return Period
Tertiary Drainage network and secondary drainage system	5 years
Primary drainage system	10 years
Box Culverts	25 years
River, Bridges and Detention Ponds	100 years

Definition of precipitation loss in a sub-basin

The precipitation loss process aims to ascertain the proportion of precipitation that passes through the earth and the proportion that turns into runoff, thereby influencing river flow. This study made use of the Soil Conservation Service (SCS) Curve Number approach. The approach was chosen mostly because the necessary characteristics for un-gauged watersheds are readily available. Developed by the Soil Conservation Service, the approach finds precipitation surplus (US Army Corps of Engineers, 2010) by combining soil cover, land use, and antecedent soil moisture. Three input values; Curve Number, Initial Abstraction, and Percentage Imperative are needed by the technique. Considered as a function of land use and soil type, the main parameter of the SCS Curve Number Method is the Curve Number (CN). The maximum precipitation the earth absorbs before runoff starts is defined by initial abstraction (Ia). Calculated as a fraction of the possible maximum retention (S), the initial abstraction is a function of the CN and represents the maximum total precipitation the ground can absorb. Equations 14 and 15 thus indicate the correlations between curve number, possible maximum retention, and initial abstraction in SI units;

$$S = \frac{25400}{CN} - 254 \quad [SI\ Units] \tag{14}$$

$$I_a = 0.2 * S$$

$$t_{Lag} = \frac{l^{0.8} * (S + 1)^{0.7}}{1900 y^{0.5}} \tag{15}$$

Definition of overland flow in a sub-basin

Termed the Transform Method in HEC-HMS, the overland flow process illustrates how the volume of excess precipitation is changed to runoff at a given location. This work applied the SCS Unit Hydrograph method. This well-established empirical approach is grounded, based on previous studies conducted in agricultural watersheds in the United States of America by Bedient *et al.* (2008) and Kalyanapu *et al.* (2009). These studies led to a relationship between the lag time and area of every sub-basin and the magnitude and timing of the peak hydrograph generated. HEC-GeoHMS computes each sub-basin's area. The lag time is the delay between the centroid of surplus precipitation and the peak of the produced hydrograph. Lag time can be obtained through numerous methods; but the two widely used approaches are the Snyder Method and the SCS Unit Hydrograph Method. Therefore, this study was carried out by applying the SCS Unit Hydrograph Method, expressed mathematically in equation 16;

$$t_{Lag} = \frac{l^{0.8} * (S + 1)^{0.7}}{1900 y^{0.5}} \tag{....(16)}$$

Where;

t_{Lag} = Basin Lag Time (hrs)

l = length from sub-basin outlet to divide along longest drainage path (ft)

y = Sub-basin slope (%)

S = 1000/CN -10 (in)

CN = Average curve number for sub-basin

Reach routing

Each real river and its tributaries were represented by a "reach" in the model. The reach routing procedure translates a hydrograph at the sub-basin's upstream border to a consequent hydrograph at the sub-basin's downstream boundary for each reach, accounting for gains and losses (energy and mass) as the river moves through that sub-basin. The form of a hydrograph inside a reach changes as it flows downstream, depending on the river channel geometry and the roughness of the surface. These characteristics influence the degree of energy loss, whereas a large channel and smooth surface result in little energy loss. However, a restricted channel with a rough surface might result in considerable energy loss. Furthermore, a steep slope accelerates flow whereas a moderate slope decelerates it. Due to time restrictions, the Muskingum-Cunge parameters were determined using the Lag technique after considerable fieldwork. Equation 17 provides a mathematical description of the lag approach.

$$O_t = \begin{cases} I_t & t < lag \\ I_{t-lag} & t \geq lag \end{cases} \tag{....(17)}$$

Where;

Lag is time by which the inflow ordinate is to be lagged; O_t is the outflow hydrographic ordinate at time t; I_t is the ordinate hydrography.

RESULTS AND DISCUSSIONS

Statistical Description of Annual Maximum Rainfall

Table 2 summarizes the statistics of the project site's annual maximum rainfall for the period spanning between 2001 and 2019. It can be inferred that maximum daily rainfall ranged from 44.43 mm to 114.89 mm and the positive skewness of 0.804.

Table 2: Statistical Summary of Maximum Daily Rainfall

Statistics	Values (mm)
Minimum	44.430
Maximum	114.896
Median	67.711
Mean	70.073
Standard Deviation	18.351
Skewness	0.804
Kurtosis	3.605

Table 3: Frequency Analysis of Maximum Daily Rainfall (2001-2019)

Annual Maximum Rainfall	M	Return period	Pr. Non-Exceedance
114.90	1	19.0	0.05
99.57	2	9.5	0.11
90.90	3	6.3	0.16
81.81	4	4.8	0.21
80.31	5	3.8	0.26
80.04	6	3.2	0.32
76.51	7	2.7	0.37
70.97	8	2.4	0.42
68.34	9	2.1	0.47
67.71	10	1.9	0.53
66.35	11	1.7	0.58
62.16	12	1.6	0.63
60.38	13	1.5	0.68
59.87	14	1.4	0.74
58.12	15	1.3	0.79
53.41	16	1.2	0.84
50.37	17	1.1	0.89
45.26	18	1.1	0.95
44.43	19	1.0	1.00

Frequency Analysis of Maximum Daily Rainfall

Table 3 shows the return periods calculated from the Hazen plotting point of the peak rainfall of the rated years between 2001 and 2019. With a low likelihood of being equaled or exceeded of 0.05, the highest storm magnitude of 114.90 mm for the research period was calculated to have a nineteen (19) year return period. Figure 1 also shows that whilst the probability of exceedance falls as reported in Table 3, the degree of peak rainfall increases as their return period grows. This suggests that although significant magnitudes of rainfalls are not regularly seen in the project region, such storms carry great hazards when they strike. Furthermore, Figure 2 demonstrates that although the plotting position was sufficient in fitting the lower left tail of the empirical rainfall distribution, it underperformed in fitting the far-right tail of the empirical distribution, which is highly crucial in reduction of flood risk. This confirms even more the importance of fitting the empirical distribution into accepted probability distribution models.

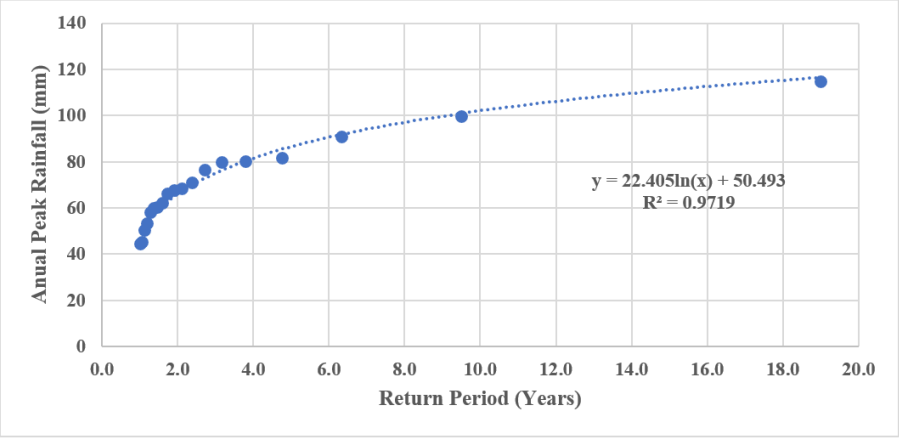

Figure 2: Probability Plot of Design storm against Return Period

Performance of Probability Distribution Models

To evaluate the adequacy of the five chosen probability distributions, GOF figures based on the AD, KS, and CM tests as well as GOF criteria like the AIC and BIC were used. In order to predict the design storms for the project area, the log-normal probability distribution with the lowest value in terms of the Anderson-Darling statistic was used, as seen in Table 4. Figure 3 shows the design storms plot for two years to a thousand years. The five return periods of interest—five, ten, twenty-five, fifty, and one hundred years—are expected to be 83.69 mm, 93.33 mm, 103.25 mm, 113.02 mm, and 130.92 mm, respectively.

Table 4: Summary of Goodness of Fit Statistics and Criteria

Goodness-of-fit statistics	Fw	Fg	Fgum	Flgn	Fnor
Kolmogorov-Smirnov statistic	0.121	0.086	0.072	0.069	0.118
Cramer-von Mises statistic	0.055	0.021	0.017	0.017	0.042
Anderson-Darling statistic	0.384	0.161	0.133	0.132	0.296
Goodness-of-fit criteria					
Akaike's Information Criterion	168.518	165.644	165.115	165.223	167.461
Bayesian Information Criterion	170.407	167.533	167.004	167.112	169.350

Fw=Weibull, Fg=Gamma, Fgum=Gumbel, Flgn=Log-normal, Fnor=Normal

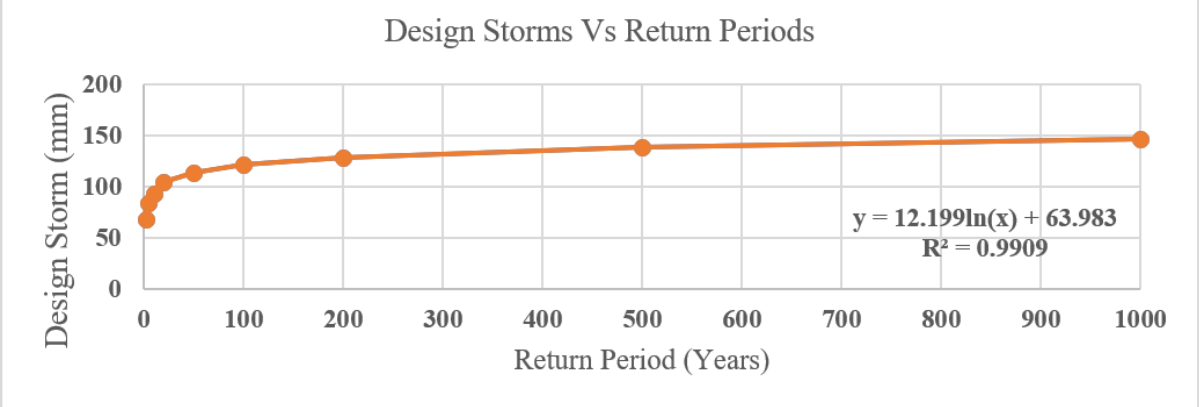

Figure 3: Probability Plot of Design storm against Return Period based on Log-Normal Distribution

Establishment of Rainfall Intensity and IDF Curve

Table 5 shows the several lengths of the 24-hour maximum daily design storms broken out. IDF normally clarifies the connection among rainfall intensity, rainfall length, and return period, thus this was done. It was important to break down the design storms into smaller periods since most rainfall statistics in Nigeria are linked to a cumulative period of 24 hours. Table 5 displays the outcome of disintegrated design storms; while Table 6 provides the related intensities.

Table 5: Summary of Disaggregated 24hr Rainfall for different durations (Minute) and Return Period

Frequency (Return Period)					
Duration	**5-year**	**10-year**	**25-year**	**50-year**	**100-year**
5min	12.90	14.38	15.91	17.42	18.64
10min	18.56	20.70	22.89	25.06	26.81
15min	16.24	18.12	20.04	21.94	23.47
30min	23.33	26.01	28.78	31.50	33.71
60min	29.32	32.70	36.18	39.60	42.37
120min	36.86	41.11	45.47	49.78	53.26
180min	42.14	46.99	51.98	56.91	60.88
360min	52.96	59.07	65.34	71.53	76.53
720min	66.58	74.25	82.14	89.91	96.20
1440min	83.69	93.33	103.25	113.02	120.93

Table 6: Summary of Disaggregated 24hr Rainfall for different durations (Hour) and Return Period

Duration (Hours)	5-year	10-year	25-year	50-year	100-year
0.083	154.77	172.61	190.95	209.02	223.64
0.17	222.70	248.36	274.75	300.76	321.79
0.25	64.98	72.46	80.16	87.75	93.89
0.5	46.65	52.03	57.56	63.01	67.41

1	29.32	32.70	36.18	39.60	42.37
2	18.43	20.55	22.74	24.89	26.63
3	14.05	15.66	17.33	18.97	20.29
6	8.83	9.84	10.89	11.92	12.76
12	5.55	6.19	6.84	7.49	8.02
24	3.49	3.89	4.30	4.71	5.04

Figure 4 shows the existing IDF curve for the project area. The established IDF estimates and curves could be further applied in hydrologic and hydraulic modeling, which are useful for drainage and bridge designs with the aim of reducing the risk of floods in the project area.

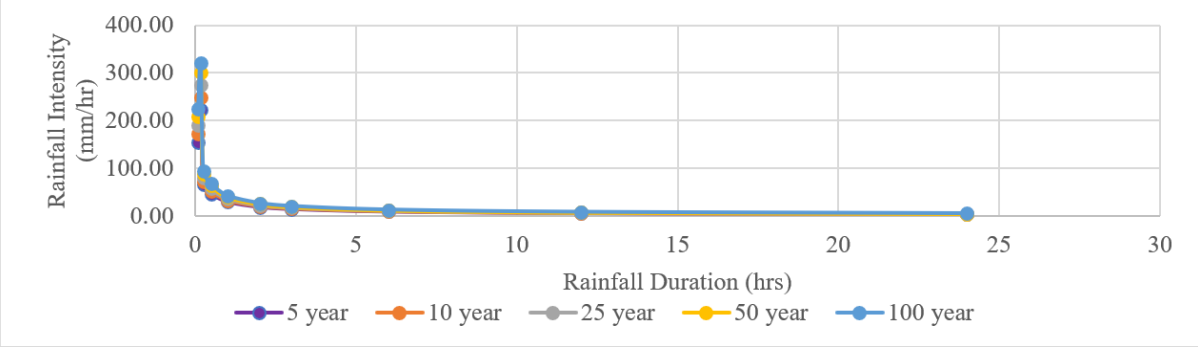

Figure 4: IDF curves for the catchment system of the proposed bridge in Kano.

Hydrologic Modeling and Simulations

Table 7 summarizes the watershed parameters used in the hydrologic simulation, and Figure 5 represents the CN distribution for the basin. Furthermore, Figure 6 represents the HMS model structures for the project region; Figure 7 depicts the hydrograph of the 100-year flood at the proposed bridge; and Table 7 summarizes the peak design flood at the proposed bridges, which serves as the hydraulic parameter for the bridge designs.

Table 7: Summary of Catchment Parameters

Basin Name	Length of the longest flow path (meters)	Drainage Slope (%)	Basin CN	Basin Lag (Hours)	Basin Slope (%)	Basin Area (Sq Km)
W200	10028.00	0.007	71.46	2.97	0.039	13.84
W210	17560.86	0.005	69.06	2.39	0.029	5.16
W220	11388.14	0.011	69.51	1.68	0.043	3.51
W230	11313.50	0.011	70.15	1.90	0.042	3.92
W240	10207.44	0.010	71.18	1.36	0.035	3.07
W250	16744.96	0.005	69.57	2.09	0.028	3.29
W260	7896.26	0.011	68.85	0.85	0.034	0.94
W270	8586.94	0.012	71.42	1.65	0.038	2.32
W280	13813.66	0.004	70.76	3.54	0.032	21.56
W290	4738.48	0.010	81.40	0.30	0.021	0.02
W300	12278.30	0.006	71.45	3.11	0.032	10.67
W310	6098.62	0.010	71.90	1.66	0.040	4.38
W320	5987.53	0.008	71.42	1.69	0.038	2.67
W330	2042.46	0.008	78.09	0.35	0.028	0.03
W340	2929.23	0.009	73.96	0.93	0.034	0.61
W350	3427.75	0.008	70.27	1.21	0.035	1.55

W360	3944.18	0.007	70.70	1.83	0.031	2.22
W370	6843.01	0.008	69.37	1.90	0.034	2.70
W380	6988.57	0.008	67.24	2.16	0.031	3.22

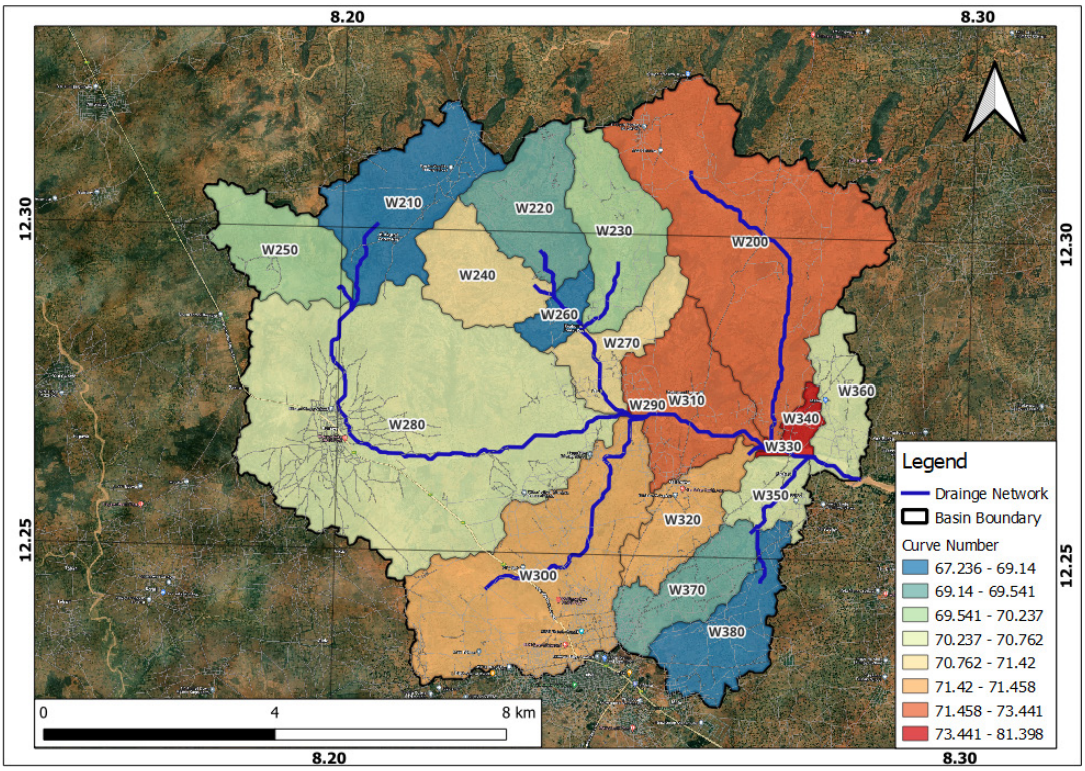

Figure 5: Curve Number (CN) for the Catchment Areas of the Proposed Bridge

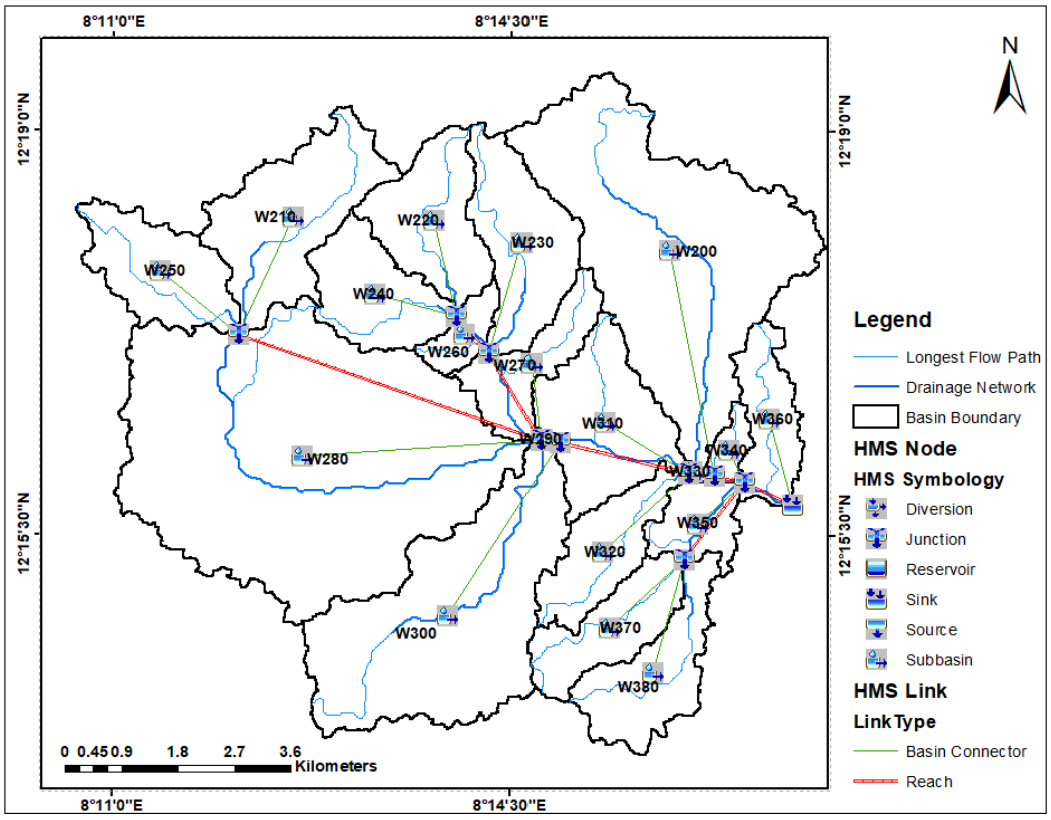

Figure 6: Hydrologic Model of Flood Discharged at the Proposed Bridge

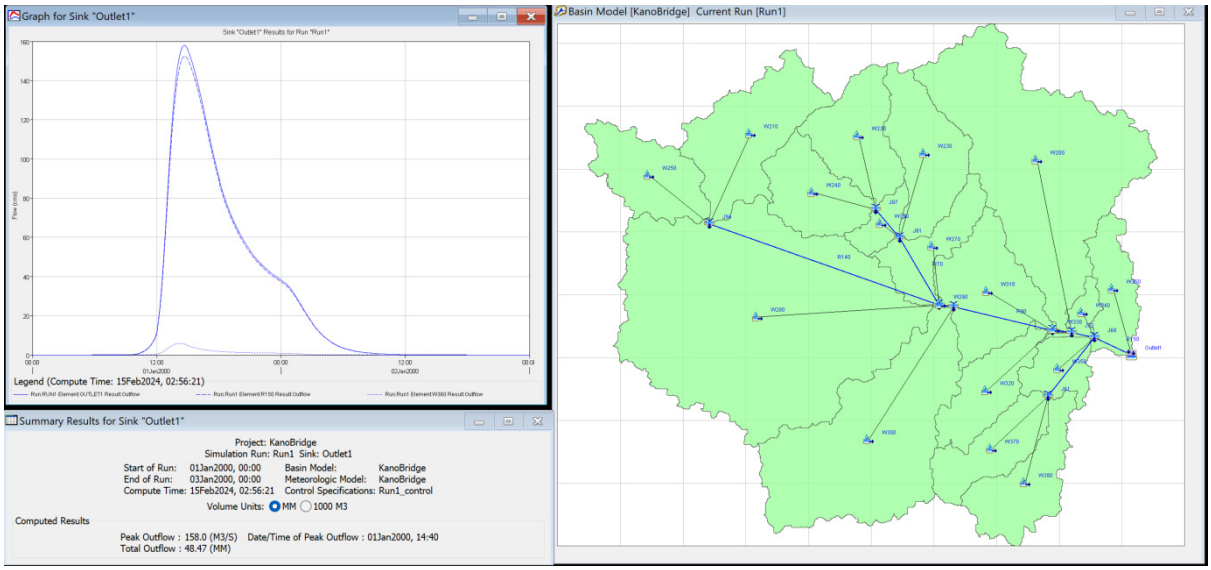

Figure 7: Hydrologic Model of Flood Discharged at the Proposed Bridge

CONCLUSION

Along with the appropriate IDF curves for the same return duration, this study produced rainfall depths for several return periods: five years, ten years, twenty five years, fifty years and one hundred years. The simulation of the peak flow of every catchment with an outlet suggested bridge location was driven by the known IDF estimations, catchment characteristics, and CN. Based on the gathered data, this study finds that the design floods are relevant for the construction of bridges in Kano State, Nigeria. Furthermore, the results obtained fit the numbers reported by Ahmed *et al.* (2021) in an earlier study conducted to determine the rainfall intensity, rainfall duration, and return period in Abuja, Nigeria, utilizing a dataset spanning 35 years.

REFERENCES

Adewale, F., & Isaac, A., (2017). Intensity, duration and frequency of rainstorms in Lokoja. *Science World Journal, 12*(2), 36-40.

Ahmed, M. A., Olowosulu, A. T., Adeogun, B. K., Murana, A. A., Ahmed, H. A., & Sanni, I. M. (2021). Development of rainfall intensity-duration-frequency (IDF) curve for Abuja, Nigeria. *Nigerian Journal of Technology, 40*(1), 154 -160.

Akpan, S., & Okoro, B. (2013). Development of intensity-duration frequency models for Calabar city, south-south Nigeria. *American Journal of Engineering Research, 2*(6), 19-24.

Alaska Satellite Facility. (2015). ASF Radiometrically Terrain CorrectedALOS PALSAR products, Product Guide, Revision 1.2, https://asf.alaska.edu

Antigha, R., & Ogarekpe, N. (2013). Development of intensity-duration frequency curves for Calabar metropolis, south-south Nigeria. *International Journal of Engineering and Sciences, 2*(3), 39-42.

Arnold, T. B., & Emerson, J. W. (2011). Nonparametric goodness-of-fit tests for discrete null distributions. *The R Journal.* https://journal.r-project.org

Bedient, P. B., Huber, W. C., & Vieux, B. E. (2008). *Hydrology and floodplain analysis.* Prentice-Hall, New Jersey.

Chowdhury, J. U., Stedinger, J. R., & Lu, L. H. (1991). *Goodness-of-fit tests for regional generalized extreme value flood distributions.* Water Resources Research. https://ui.adsabs.harvard.edu

Fadipe, O. O., Adeosun, J. O., Adeyanju, K. O., & Oguntola, M. O. (2020). Characteristics of packaged water under different storage conditions within Osogbo metropolis. *Uniosun Journal of Engineering and Environmental Sciences, 2*(2), 87-97.

Hassan, A. S., Elgarhy, M., Mohamd, R. E., & Alrajhi, S. (2019). On the alpha power transformed power lindley distribution. *Journal of Probability and Statistics, 3*(5), 45-61.

Ilaboya, I. R., & Nwachukwu, S. N. (2022). Development of intensity duration frequency (IDF) curves for rainfall prediction in some selected states in south-west Nigeria. *Journal of Energy, Technology and Environment, 4*(2), 69-82.

Isah, H. M., Sawyerr, H. O., Raimi, M. O., Bashir, B. G., Haladu, S., & Odipe, O. E. (2020). Assessment of commonly used pesticides and frequency of self-reported symptoms on farmers' health in Kura, Kano State, Nigeria. *Journal of Education and Learning Management, 1*(1), 31-54.

Kalyanapu, A. J., Burian, S. J., & McPherson, T. N. (2009). Effect of land use-based surface roughness on hydrologic model output. *Journal of Spatial Hydrology, 4*(9), 51-71.

Laio, F., (2004). Cramer-von Mises and Anderson-Darling goodness of fit tests for extreme value distributions

with unknown parameters. *Water Resources Research, 40*(9), 24-40.

Langat, P. K., Kumar, L., & Koech, R. (2019). Identification of the most suitable probability distribution models for maximum, minimum and mean stream flow. *Water, 11*(4), 734–756.

National Aeronautics and Space Administration. (2018). *Global precipitation measurement integrated multi-satellite retrievals for gpm (IMERG).* https://gpm.nasa.gov/data/imerg

Nwaogozie, I. L., & Okonkwo, S. C. (2017). Rainfall-intensity-duration-frequency modeling and comparative analysis of developed models for Abakaliki, Ebonyi State, Nigeria. *International Journal of Trends in Research and Development, 4*(2), 45-53.

Nwaogozie, I., & Ekwueme, M. C. (2017). Rainfall intensity-duration (IDF) models for Uyo city, Nigeria. *International Journal of Hydrology, 1*(3), 63-66.

Obot, N. I., Chendo, M., Udo, S., & Ewona, I. (2010). Evaluation of rainfall trends in Nigeria for 30 years (1978-2007). *International Journal of the Physical Sciences, 5*(14), 2217-2222.

Oladejo, O. S. (2014). *Fundamentals of environmental engineering, handbook of environmental engineering, Ogbomoso, Oyo State.* Olanrewaju Publishers.

Oladejo, O. S., & Olanipekun, A. A. (2018). Phyto-remediation of municipal run-off using typha orientalis and sorghum arundinaceum in sub-surface constructed wetland system. *International Research Journal of Advanced Engineering and Science, 3*(1), 211–215.

Olanipekun, A. A., & Idusuyi, D. U. (2023). Design and construction of bio-sand filtration system for treatment of influent obtained from a well and stream. *International Journal of Scientific and Engineering Research, 14*(3), 1–15.

Rasel, M. M., & Islam, M. (2015). Generation of rainfall-intensity duration frequency relationship for north-western region in Bangladesh. *IOSR Journal of Environmental Science, Toxicology and Food Technology, 9*(9), 41-47.

Sule, B. F., & Ige, K. (2016). Synthesis of isopluvial maps for Nigeria using IDF equations derived from daily rainfall data. *Journal of Scientific and Engineering Research, 3*(3), 505-514.

U.S Army Corps of Engineers (2010). *Engineer research and development center.* Wetlands Regulatory Assistance Programme. https://www.nap.usace.army.mil

World Health Organization. (WHO) (2022). *Guidelines for drinking-water quality, health criteria and other supporting information.* https://iris.who.int.